BMC Pulmonary Medicine

RESEARCH

Open Access

Genome-wide analysis of m6A-modified circRNAs in the mouse model of myocardial injury induced by obstructive sleep apnea

Jiuhuang Lan[1,2*†], Yuhui Wang[1,2†], Chang Liu[1,2], Hongli Chen[1,2] and Qingshi Chen[3*†]

Abstract

Background The peculiar expression of N6-methyladenosine (m6A) in Circular RNAs (circRNAs) is closely linked to the occurrence of many diseases. However, roles of m6A-modified circRNAs in OSA-induced cardiovascular disease are unknown. Here, we use bioinformatics analysis to investigate the expression profiles of m6A-modified circRNAs and reveal their potential functional roles in the mouse models of chronic intermittent hypoxia (CIH).

Methods Firstly, the expression profiles of m6A-modified circRNA in left ventricular tissue of the CIH mouse model were examined using circRNA microarray analysis. Then, the expression level of selected circrRNA was compared by folding change filtration, and the consistency between them and microarray results was verified by MeRIP-qPCR. GO analyses and KEGG analyses were conducted to predict the potential functions of these m6A-modified circRNAs. Finally, we conducted a ceRNA analysis, and a network was constructed to clarify the relationship between the selected circRNAs and miRNAs as well as the targeted genes.

Results In total, 255 circRNAs with m6A peaks in CIH-treated cardiac tissues were identified. 250 were up-regulated, 5 were down-regulated. The results of MeRIP-qPCR were consistent with the microarray results. 73 pathways were detected in the up-regulated transcripts and no relevant pathways were detected in the down-regulated transcripts. Finally, three circRNAs (mmu_circRNAs_22543, mmu_circRNAs_29768, and mmu_circRNAs_34841) were selected for ceRNA analysis, and the circRNA-miRNA-mRNA network was constructed.

Conclusion Our findings are the first to show that m6A-modified circRNAs play a key role in OSA-induced cardiovascular disease. This study highlights the pivotal role of m6A-modified circRNAs in regulating gene expression and their potential implications in understanding the molecular pathogenesis of OSA-induced cardiac injury.

Keywords CircRNAs, N6-methyladenosine(m6A), Obstructive sleep apnea, Chronic intermittent hypoxia (CIH), Cardiovascular disease, Bioinformatics analysis

†Jiuhuang Lan, Yuhui Wang and Qingshi Chen contributed equally to this work.

*Correspondence:
Jiuhuang Lan
lanjiuhuang2001@163.com
Qingshi Chen
chenqingshi1986@126.com

[1]The Second Clinical Medical College, Fujian Medical University, Quanzhou, China
[2]The Second Affiliated Hospital of Fujian Medical University, No.950 Donghai Street, Fengze District, Quanzhou 362000, China
[3]Department of Endocrinology and Metabolism, The Second Affiliated Hospital of Fujian Medical University, No.950 Donghai Street, Fengze District, Quanzhou 362000, China

Introduction

Obstructive sleep apnea (OSA) is a frequent medical condition characterized by sleep-disordered breathing with episodes of sectional or complete obstruction of the upper airway, which causes sleep fragmentation, autonomic instability, and occasional hypoxemia [1]. OSA affects about 10% of adults, but the great majority of them don't attach importance to it [2]. OSA is regarded as a risk factor for conditions including hypertension, coronary artery disease, stroke, congestive heart failure, pulmonary hypertension, and cardiac arrhythmias [2, 3]. Potential mechanisms include sympathetic activation, oxidative stress, and inflammation [4]. Numerous prevalent risk factors and concomitant circumstances that raise the risks of cardiovascular disease (CVD) alone are also connected to OSA, including metabolic syndrome and hyperlipidemia [5]. Based on this, studying the unique pathophysiology of OSA and cardiovascular illness as well as the precise possible mechanism underlying their connection is crucial.

Circular RNAs (circRNAs) are a brand-new class of non-coded RNAs. There are some studies reporting that these circRNAs could be essential to numerous cellular processes [6, 7]. Recent research has revealed that circRNAs interact with microRNAs (miRNAs), forming circRNA-miRNA axes that regulate disease-related genes [8]. These interactions are implicated in diseases such as carcinogenesis [9], myocardial infarction [10], and bone-related diseases [11]. The process of adding one or two dimethyl groups to certain nucleotide residues in RNA is known as RNA methylation, such as N1-methyladenosine (m1A) and 5-methylcytosine (m5C) [12, 13]. Among these modifications, one of the most common alterations is N6-methyladenosine (m6A) [14]. Researchers have conducted many analyses on the mechanism of m6A modification [15]. For instance, highly conserved methyltransferases (writers), demethylases (erasers), and binding proteins all work together to catalyze the m6A modification process (readers) [16, 17]. For instance, AML destroys normal cell differentiation through m6A modification, thus promoting cancer development [18]. m6A modifications are crucial post-transcriptional regulators, and emerging evidence links circRNAs to heart disease. Understanding these modifications in OSA-induced injury opens new therapeutic possibilities. Although substantial progress has been made in the field of RNA methylation related to m6A-modified RNAs, the mechanism of m6A methylation in mouse models of OSA-induced cardiac injury has not been investigated. And the relationship between m6A methylation and OSA-induced myocardial injury is still unclear.

In the current study, we first identified the expression profiles of m6A-modified circRNAs in the left ventricular tissues of the chronic intermittent hypoxia (CIH) animal models using circRNA microarray analysis. Following that, the reliability of the microarray chip results was verified by MeRIP-qPCR to provide the basis for our experiments. Meantime, Gene Ontology (GO) analyses and Kyoto Encyclopedia of Genes and Genomes (KEGG) pathway analyses were conducted to predict the potential functions of these m6A-modified circRNAs. Finally, we conducted the ceRNA analysis on the alternative circRNAs screened by the microarray, a network was constructed to elucidate the relationship between the chosen circRNAs and miRNAs as well as targeted genes. Our findings lay the groundwork for future studies on m6A-modified circRNAs in OSA-related heart disease and raise the possibility that m6A-methylated circRNAs may be associated with the development and incidence of OSA-induced cardiac damage.

Materials and methods

Animal models

Beijing Weitong Lihua Experimental Animal Technology Co., Ltd. provided male Balb/c mice (17–21 g, 6 weeks old). The National Institutes of Health Guide for Laboratory Animals was followed for performing animal research. The animal protocol for this work was approved by the Second Affiliated Hospital of Fujian Medical University's Experimental Animal Ethics Committee. All methods were performed in accordance with relevant guidelines and regulations.

Simply put, considering potential mortality during chronic intermittent hypoxia exposure, we randomly assigned the 18 mice listed above to 2 groups. There were 9 mice in the CIH group and 9 mice in the control group, and the dead mice were excluded as the experiment progressed. Last, 3 mice were chosen at random from each group to participate in the experiment. Mice were housed in a temperature-controlled environment with a 12-hour light/dark cycle to minimize stress during the experiments. The control group was housed in a chamber with an oxygen concentration of 21% throughout the experiment. And the CIH group was put into the specially designed, commercially intermittent hypoxia system (ProOx-100-CIH-M, Shanghai TOW Intelligent Technology Co., Ltd). In the first 60 s, nitrogen was transported to the container in order to reach 6% oxygen, which could provide an environment for hypoxia. In the last 60 s, oxygen was delivered to the container for the purpose of reaching 21% O^2. With the assistance of an oxygen analyzer, the oxygen concentration was computed automatically. The hypoxia chamber was monitored continuously to maintain precise oxygen levels and avoid unnecessary stress to the animals. Recovery periods were provided between hypoxia cycles. The above operations constituted one cycle. It lasts for eight weeks, 30 cycles a day for a total of eight hours. Euthanasia was

performed using cervical dislocation following guidelines from the ARRIVE 2.0 framework, ensuring a humane and ethical endpoint. Then, their left ventricular tissues were collected.

Take myocardial samples and HE pathology

After the mice were euthanized, the ventricular tissue was retrieved, treated with 4% formaldehyde, and then embedded in paraffin. Subsequently, we stained all the 5-μm-thick slices with hematoxylin and eosin to look for alterations in the overall cell morphology in the myocardial tissues. In the end, we carefully inspected the sections under an optical microscope with a 400x magnification to make an accurate pathology diagnosis.

Quantification of m6A-RNA Immunoprecipitation and purification

The total RNAs were immunoprecipitated using an anti-N6-methyladenosine (m6A) antibody. Polysome lysis buffer was used to lyse total RNA and m6A-peak control mixture, then cleavage product was gleaned. After attaching the anti-m6A rabbit polyclonal antibody (Synaptic Systems) to the encapsulated magnetic beads, the mixture was immunoprecipitated by incubating with protein-A beads for 2 h at 4 °C. In each sample, 20 μL Dynabeads™M-280 Sheep Anti-Rabbit IgG suspension was blocked at 4℃ for 2 h and then re-suspended in a previously prepared total RNA antibody mixture. The washing solution and 1xlP buffer solution were used for treatment, then elution buffer was used to extract and enrich RNA. Finally, the RNA was then extracted with acid phenol chloroform and precipitated with ethanol. The modified RNAs were extracted using the "IP"—immunoprecipitated magnetic beads. The unmodified RNAs, referred to as "Sup," were recovered from the supernatant. Following the addition of an equal quantity of calibration spike-in control RNA, the enriched "IP" and "Sup" RNAs were amplified independently and labeled with Cy3 (for "Sup") and Cy5 (for "IP") using the Arraystar Super RNA Labeling Kit. The purity and amount of total RNA sample were determined using the NanoDrop ND-1000 (pmol dye/μg cRNA). RNA integrity was assessed using the Bioanalyzer 2100 or Mops electrophoresis. The generated cRNAs were purified using the RNeasy Mini Kit.

CircRNA microarray hybridization

The Arraystar standard methodology was followed for sample preparation and microarray hybridization. The "IP" and "Sup" RNAs were subjected to RNase R treatment before being individually tagged with Cy5 and Cy3 as cRNAs in accordance with the Arraystar RNA Labeling technique to remove linear RNAs and enrich circular RNAs. After the cRNAs were concatenated, they were hybridized in an Agilent Hybridization Oven at 65 °C for 17 h using the Arraystar Mouse CircRNA Epitranscriptomic Arrays (8 × 15 K, Arraystar). After cleaning the slides, an Agilent Scanner G2505C was used to scan the arrays in two-color channels. The Limma R package's quantile normalization was used to standardize the raw signal intensities, and the Benjamini-Hochberg FDR correction was used to assess statistical significance.

Microarray data analysis

Using Agilent Feature Extraction software, the acquired array pictures were examined. The IP (Cy5-labelled) normalized intensities were used to determine the "m6A quantity," or the amount of m6A methylation in each transcript. In the meantime, the IP (Cy5-labelled) and Sup (Cy3-labelled) normalised intensities were used to compute the percentage of m6A methylation (%Modified) for a transcript. We also employed the R software's Limma package for quantile normalization and further data processing. The Fold fold change (FC) ≥ 2 and P values < 0.05 were used to determine statistical significance for circulating RNAs in order to compare two groups for differential m6A modification. The Data/Sort and Filter features in Microsoft Excel can be used to further rank the differentially m6A-methylated circRNAs and modify the stringency thresholds. The samples were sorted according to how similar their m6A methylation levels or amounts were and how closely related they were. To identify the differentially changed circRNAs between the two groups, fold-change filtering was used. To illustrate the distinctive circRNA-expression patterns among the samples, hierarchical clustering was also used. the volcano plot and the scatter plot described the differences in the expression of m6A-modified circRNAs between the two groups.

GO annotation and KEGG pathway enrichment analyses

To learn more about the biological activities of the genes in the substantially connected module, we performed GO analysis and KEGG pathway enrichment analysis for the host genes of the selected circRNAs with m6A peaks. Cellular component (CC), molecular function (MF), and biological process (BP) categories were included. The important routes all have a p-value of less than 0.05.

MeRIP-qPCR

Real-time qPCR was carried out using the $2^{-\Delta\Delta Ct}$ technique to examine the enrichment of m6A-modified RNA, and the m6A-RIP fraction normalized to the input was determined. The samples were extracted and then utilized to build the library on the HiSeq 4000 using Prep Kit (Illumina). The primers were shown in Table 1.

Table 1 Primers used for MeRIP-qPCR

Genes	Sequence	Tm (℃)	Lengths (bp)
mmu_circRNA_011180	F:5′-ACTGCGCAAGAGA-AAGTGG-3′ R:5′-CTCAAAGGGATG-GAAGTCG-3′	60	95
mmu_circRNA_014597	F:5′-CTTCAATGATTTTCACCTC-CAG-3′ R:5′-AGCGGTCATCCATGCT-TATAT-3′	60	123
mmu_circRNA_008397	F:5′-GATGCGTTTTCACAGGC-TACA-3′ R:5′-TCTCCAGACAGAACCTC-CAGG-3′	60	299
mmu_circRNA_34841	F:5′-AGATTTGTAGTTC-CAGAAAGGTG-3′ R:5′-GCTCCAATCAGAGATGC-TACTT-3′	60	155
mmu_circRNA_22543	F:5′-CTTAACAGGTCGTA-AGAGTGAGGC-3′ R:5′-GTAGAAAATGTGTGTC-CAGGGG-3′	60	150
mmu_circRNA_29768	F:5′-TATGACGAAACGGTA-ACCCAC-3′ R:5′-GGATAACAGACTGCAGAT-CAAGC-3′	60	157

Construction of a CeRNA interaction network

To construct the circRNA-miRNA-mRNA network, we chosen three significantly differentially expressed circRNAs modified by m6A by software (Arraystar's in-house miRNA target prediction software), which was based on miRanda and TargetScan. This ceRNA network represents a predictive model derived from computational analysis, providing insights into potential regulatory interactions. Then, we used Cytoscape for 3 chosen circRNAs and all differentially expressed mRNAs as well as targeted genes to build a competitive endogenous RNA (ceRNA) network (commonNum >= 3, context+ < -0.15, Structure > 140). Cytoscape with a Pearson correlation coefficient (r) > 0.97 was utilized to depict the CNC network.

Statistical analysis

Through using R version 4.0.2, we carried out at least three separate repeated experiments and conducted all statistical analysis of the data. The means standard deviation of several m6A modification subclusters were shown. The fold change (FC) was calculated using normalized microarray signal intensities, and significance was tested using a two-tailed Student's t-test for two-group comparisons. For pathway enrichment analysis (GO and KEGG), we employed the hypergeometric test, with p-values adjusted using the Benjamini-Hochberg method for multiple comparisons (FDR < 0.05). To show a statistically significant difference, a $P < 0.05$ test was used.

Results

Observation of myocardial histological changes

To ascertain whether the heart tissue in the CIH group had sustained any damage, histological abnormalities in the control group and the CIH group were identified using hematoxylin and eosin staining, respectively. After viewing the magnified image under the microscope, no significant changes were observed in the left ventricular myocardium of the control group (Fig. 1A). The abnormal myocardial structure, myocardial cell atrophy, and nuclear deformation in the CIH group were prominent (Fig. 1B).

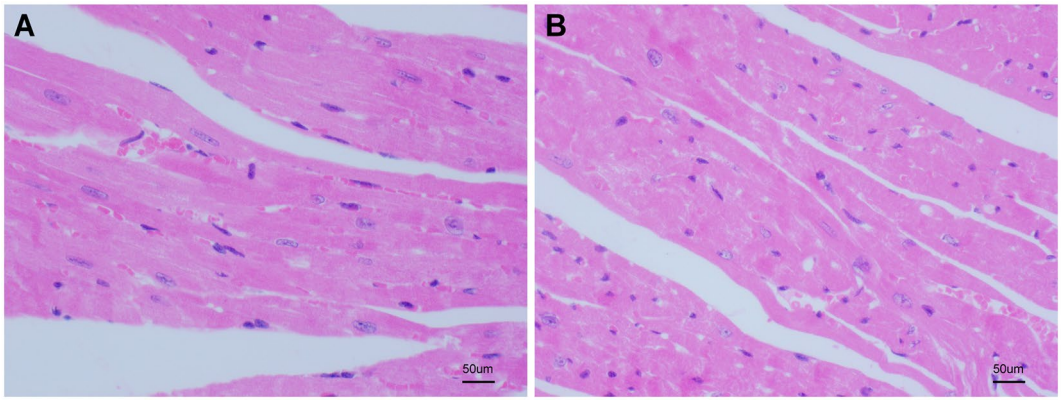

Fig. 1 Effect of CIH on the histopathology of myocardium. (**A**) Myocardial tissue from control group mice (normoxia) shows intact and well-organized myocardial architecture, with normal cell morphology and nuclei. The cells are uniformly distributed, and no signs of inflammation or fibrosis are observed. (**B**) Myocardial tissue from CIH-treated mice exhibits significant abnormalities, including distorted myocardial structure, nuclear deformation, and noticeable atrophy of myocardial cells. The tissue shows signs of inflammation and fibrosis, indicating pathological changes induced by chronic intermittent hypoxia. Hematoxylin and eosin staining was used to visualize the tissue morphology at 400x magnification

Identification of m6A-modified circrnas in the animal model of OSA

We calculated the fold change (FC) and statistical significance of the difference (P value) for each transcript in order to compare two groups (the CIH groups and controls) for differential m6A modification. The default threshold was set to|FC| ≥ 2, and the *P*-values were set to $P < 0.05$. Six samples (three samples in the CIH group and the other three samples in the control group) were selected for the microarray analysis. According to the criteria of|FC| threshold ≥ 2 and $P < 0.05$, 255 differentially expressed m6A-modified circRNAs were detected in our OSA-induced heart damage mouse model. Among them, 250 circRNAs were found significantly up-regulated, and 5 circRNAs were found significantly down-regulated.

To ensure the high quality of the microarray data, we applied hierarchical clustering heatmap analysis to all differentially expressed circRNAs, which were shown in Fig. 2A. The heatmap showed that the circRNA expression profiles between the CIH and the control tissues significantly differed. Furthermore, the volcano plot and the scatter plot described the differences in the expression of m6A-modified circRNAs between the CIH and control groups (Fig. 2B, C). Meanwhile, we selected three significantly differentially expressed circRNAs (mmu_circRNAs_22543, mmu_circRNAs_29768, and mmu_circRNAs_34841) for ceRNA analysis to construct a ceRNA network, which enabled us to seek novel pathways and targets.

GO analysis of m6A-modified circrnas with significant differential expressions

To investigate the critical functions of the object genes in the biological and pathological meanings of m6A methylation in myocardial injury induced by OSA, GO enrichment analysis of the host genes of the selected circRNAs with m6A peaks was performed. In the up-regulated transcripts, a total of 1319 biological processes (BP), 183 cellular ingredients (CC), and 160 molecular functions (MF) were identified via GO analysis. For the down-regulated transcripts, a total of 173 biological processes (BP), 20 cellular ingredients (CC), and 46 molecular functions (MF) were identified We ranked the top five in each category based on the p-value from smallest to largest and plotted the graph (Fig. 3). The transcripts of up-regulated were enriched in cellular process (Fig. 3A, BP), organelle (Fig. 3A, CC), and binding (Fig. 3A, MF). The transcripts of down-regulated were enriched in G1 to G0 transition (Fig. 3B, BP), chromatin silencing complex (Fig. 3B, CC), and transferase activity (Fig. 3B, MF).

Prediction of pathways

KEGG pathway analysis was conducted to identify multiple pathways of OSA-induced heart damage associated with m6A-modified circRNAs. We performed pathway analysis for the host genes of selected circRNAs with m6A peaks. In our study, a total of 73 pathways were detected in the up-regulated transcripts with $P < 0.05$, but the pathways could not be identified in the down-regulated transcripts. Then we selected the top 10 pathways from the results based on the magnitude of the p-value values and drawn the Sankey diagram according to the counts of DE genes from small to large (Fig. 4). The transcripts of the m6A-modified circRNAs were significantly associated with the pathways in cancer, the focal adhesion, the proteoglycans in cancer, the phospholipase D signaling pathway, the thyroid hormone signaling pathway, and the AMPK signaling pathway. Figure 4 showed that the genes such as ADCY5, CTNNA1, and HIF1A are associated with the pathways in cancer, whereas the genes such as FLNB, IGF1R, CTNNB1, and LAMB2 were involved in the focal adhesion.

Verification of m6A-RNA Immunoprecipitation and MeRIP-qPCR

We used MeRIP-qPCR to detect the expression levels of six selected circRNAs with m6A peaks. The results demonstrated that three up-regulated circRNAs (mmu_circRNAs_011180, mmu_circRNAs_014597, and mmu_circRNAs_008397) and three down-regulated circRNAs (mmu_circRNAs_34841, mmu_circRNAs_22543, and mmu_circRNAs_29768) identified through MeRIP-qPCR showcased a similar trend of expression (Fig. 5). This result demonstrated the trustworthiness of our m6A-modified circRNA-seq data.

Prediction of relevant targeted genes and pathways

To explore the m6A-modified circRNA-miRNA-mRNA network, we used TargetScan and miRanda to predict the circRNA targets and downstream genes with abnormal regulation. Then, in order to elucidate the biological function of m6A-modified circRNAs in OSA-induced cardiac injury, a ceRNA interaction network was constructed by Cytoscape software. A total of three circRNAs (mmu_circRNAs_22543, mmu_circRNAs_29768, and mmu_circRNAs_34841) and their targeted genes were chosen. The network constructed was illustrated in Fig. 6.

In this network map, several important mRNAs that participated in the occurrence and development of OSA were found to bind to these m6A-modified circRNAs. For instance, mmu-miR-5134-5p, mmu-miR-1896, and mmu-miR-7242-3p as well as their respective targeted genes were predicted to have a pathway linkage with mmu_circRNA_22543. In addition, Clip2, Fadd, and Hacd2 genes were associated with mmu_circRNA_22543.

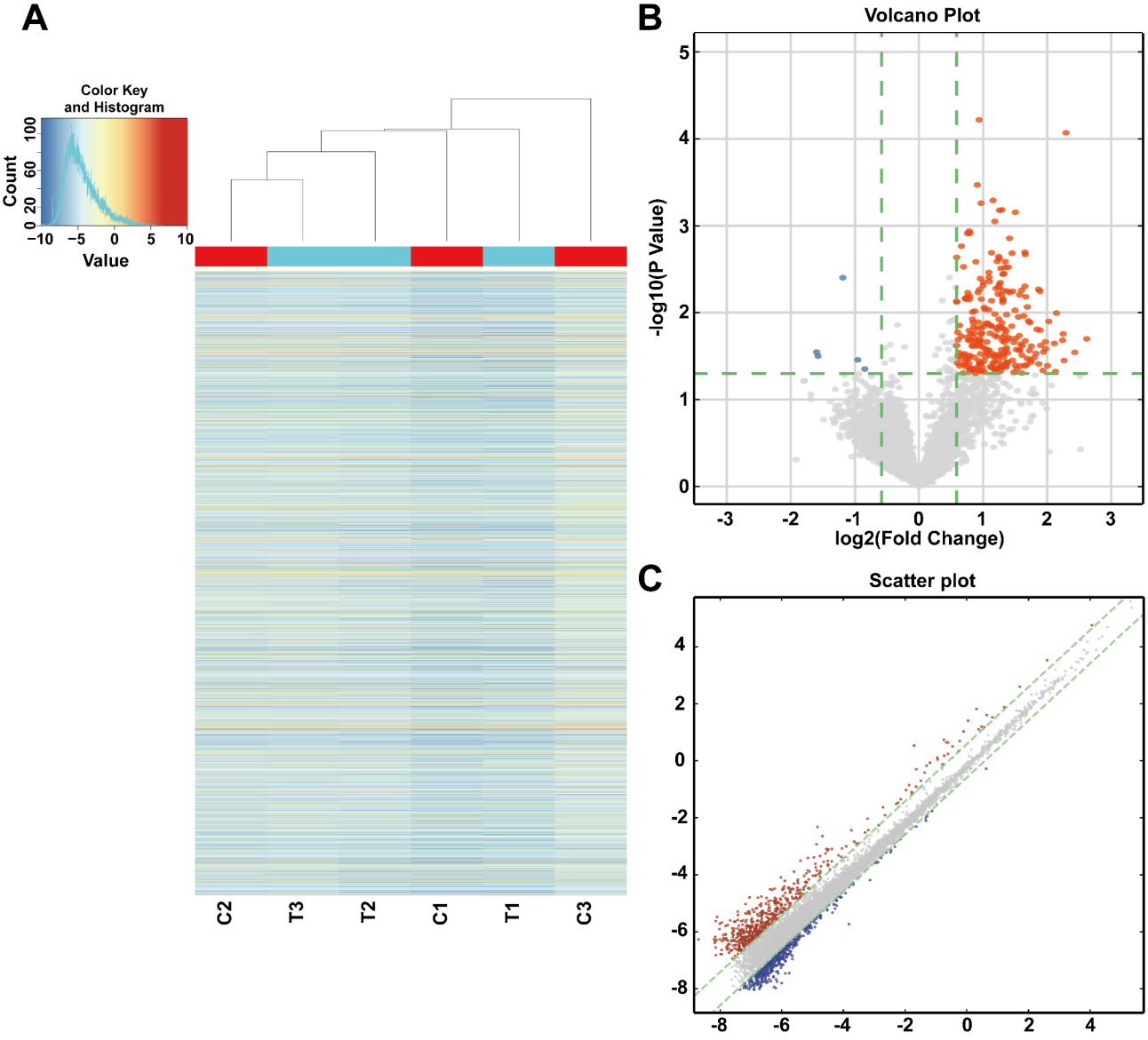

Fig. 2 Differential expression analysis of m6A-modified circRNAs in CIH and control groups. **A** Heatmap of differentially expressed circRNAs modified by m6A, showing hierarchical clustering of samples from CIH and control groups. Red indicates up-regulated circRNAs, and blue indicates down-regulated circRNAs ($|FC| \geq 2$, $p < 0.05$). The heatmap demonstrates clear separation between the CIH and control groups, indicating distinct expression patterns. **B** Volcano plot showing the distribution of circRNAs based on fold change and statistical significance. Up-regulated circRNAs are shown in red, and down-regulated circRNAs are shown in blue, with gray dots indicating non-significant changes. The plot highlights the significant differences in circRNA expression between the two groups. **C** Scatter plot of normalized signal intensities of circRNAs in the two groups, highlighting the distribution of differentially expressed m6A-modified circRNAs ($|FC| \geq 2$, $p < 0.05$). The scatter plot illustrates the overall expression trends and the degree of variation between the groups

Discussion

According to our knowledge, this study is the first to describe the expression profiles of circRNAs modified by m6A in the mouse model of myocardial damage induced by OSA. In addition, a few potential targets and pathways of circRNAs with m6A peaks involved in heart damage were shown in our study. What's more, this work expanded our understanding of the roles of m6A-modified circRNAs in myocardial diseases induced by OSA and attempted to describe their significance.

As a common disorder, OSA is characterized by repeated apnea or frequent hypopnea during sleep, resulting in decreased saturation and frequent awakenings [1]. Severe OSA may increase the risk of other comorbidities with adverse medical outcomes, such as cardiovascular and cerebrovascular disease, diabetes mellitus, depression, dementia, and even some types of

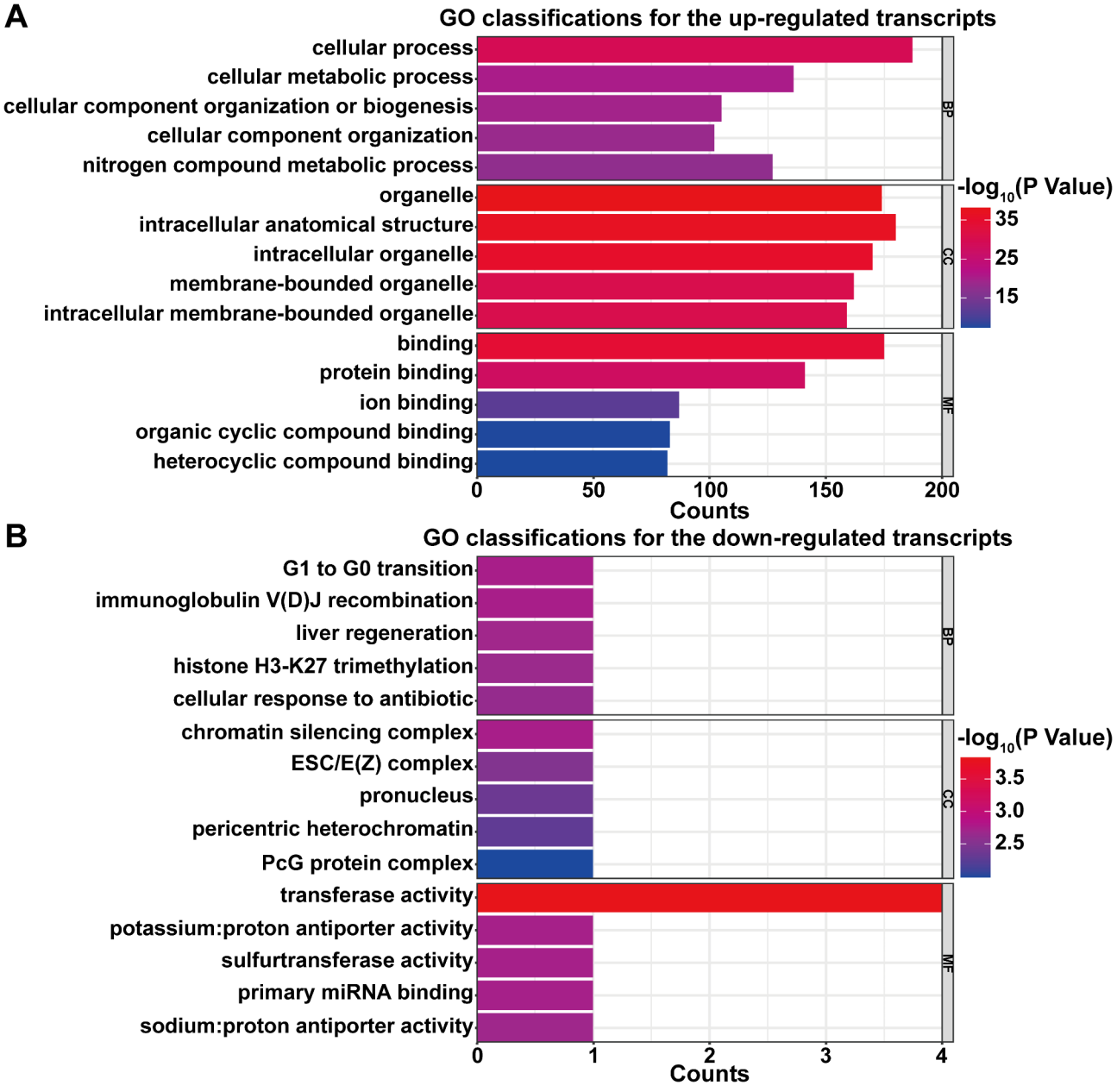

Fig. 3 GO enrichment analysis of host genes for m6A-modified circRNAs. **A** Top five enriched GO terms for up-regulated transcripts are displayed in three categories: biological processes (BP), cellular components (CC), and molecular functions (MF). Significant terms include 'cellular process' (BP), 'organelle' (CC), and 'binding' (MF). **B** Top five enriched GO terms for down-regulated transcripts, including 'G1 to G0 transition' (BP), 'chromatin silencing complex' (CC), and 'transferase activity' (MF). The bars represent the level of enrichment significance based on p-value

cancer [19–22]. OSA is considered a major cause of heart damage, as evidenced by numerous studies [23]. However, there are still some obstacles to the study of the relationship between OSA and cardiovascular diseases. For example, patients who are diagnosed with cardiovascular diseases induced by OSA often have a few risk factors such as smoking, diabetes mellitus, and obesity, and it is difficult to define the single mechanism of OSA induction. And it often takes years for OSA patients to have cardiovascular diseases diagnosed clinically, so changes in the condition can be challenging to detect. Due to these risk factors, macroscopic studies of the causal relationship between OSA and cardiovascular diseases are limited, driving research toward molecular and epigenetic targets.

CircRNAs have attracted increasing attention due to their wide expression in various diseases, especially cardiac diseases, and their potential association with pathogenic mechanisms [24]. For example, Garikipati et al. detected that circRNA expression levels changed in

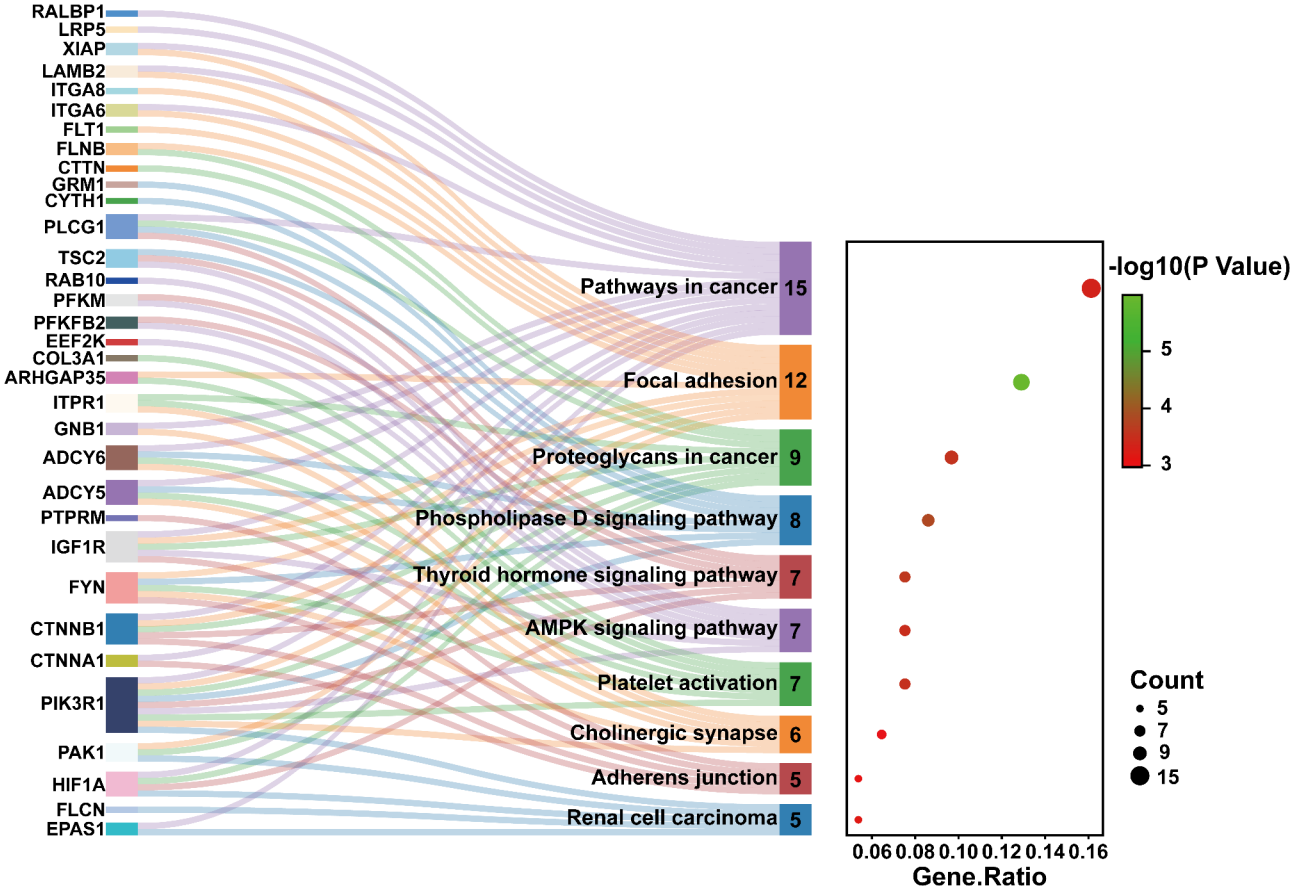

Fig. 4 KEGG Pathway Enrichment Analysis of m6A-modified circRNAs. The Sankey diagram represents the enriched KEGG pathways linked to differentially expressed m6A-modified circRNAs in the OSA-induced cardiac injury model. The pathways shown, such as the AMPK signaling pathway, focal adhesion, and proteoglycans in cancer, are among the top 10 enriched pathways with a significant involvement in myocardial injury. Each pathway is annotated with the associated genes, including CTNNA1, FLNB, and HIF1A, which play a crucial role in cardiac pathophysiology. The diagram also shows the ratio of differentially expressed genes (DE genes) to the total number of genes in each pathway, providing a visual summary of the functional roles of these circRNAs in OSA-induced cardiovascular damage. Color-coded pathways highlight the strength of enrichment, with red indicating pathways most significantly affected by the circRNAs

a mouse model of post-myocardial infarction [25]. Ge et al. showed for the first time that 185 circRNAs were drastically differently expressed in the pathogenic and pathophysiological processes of ischemia/reperfusion heart damage [26]. In recent years, researchers have found that m6A methylation of circRNAs is pervasive in epigenetics-related research fields [27]. Some researchers have discussed the role of m6A modification in circRNA expression and metabolism, and there is a growing consensus that m6A-modified circRNAs play vital roles in the development of some diseases [28–33]. For instance, Chen R et al. reported that m6A-methylated circNSUN2 may promote the progression of colorectal cancer [28]. Berulava et al. reported that the expression of m6A-modified RNAs was altered in cardiac hypertrophy and heart failure [34]. However, the mechanisms and targets of m6A-modified circRNAs in OSA-induced myocardial injury remain unclear. So, we used the CIH mouse model to demonstrate the potential mechanisms of m6A-modified circRNAs in OSA-induced myocardial injury.

To fully elucidate the expression profiles of m6A-modified circRNAs, we conducted microarray analysis. We identified 255 differentially expressed m6A-modified circRNAs, with 250 upregulated and 5 downregulated. To validate these findings, we performed MeRIP-qPCR on six selected circRNAs, all of which showed statistically significant results consistent with the microarray data. Nevertheless, the specific biological functions of these circRNAs and the related genes and pathways remain to be elucidated.

To predict the biological roles and possible targets of circRNAs with m6A peaks in the progression of OSA-induced cardiac injury, we conducted GO and pathway analyses. The results of the GO analysis showed that the transcripts of up-regulated were germane to cellular process, organelle, and binding, and the transcripts of down-regulated were enriched in G1 to G0 transition,

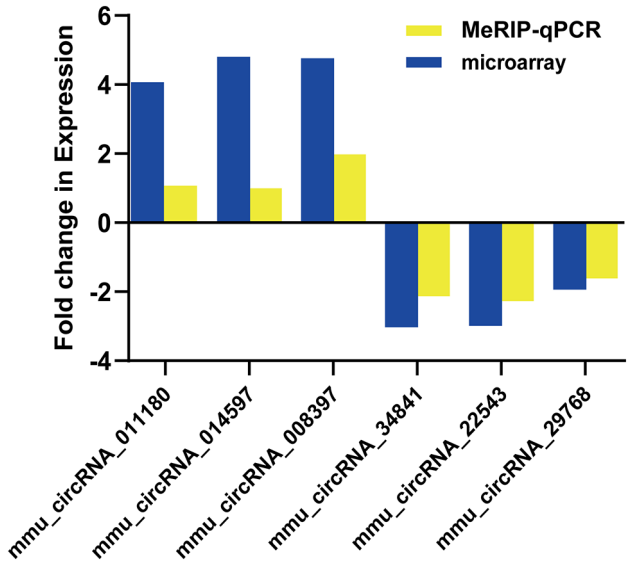

Fig. 5 Validation of microarray results using MeRIP-qPCR for six candidate circRNAs. Three up-regulated circRNAs (mmu_circRNAs_011180, mmu_circRNAs_014597, mmu_circRNAs_008397) and three down-regulated circRNAs (mmu_circRNAs_34841, mmu_circRNAs_22543, mmu_circRNAs_29768) were assessed. Bar plots represent the normalized expression levels of these circRNAs, showing trends consistent with the microarray data. Statistical significance was determined using Student's t-test ($p < 0.05$)

chromatin silencing complex, and transferase activity. Using the gene ontology knowledgebase, we identified genes linking cellular metabolism to immunity, such as IRGM, which encodes a protein involved in antiviral responses. In addition, among the downregulated results, we queried the term of immunoglobulin V(D)J recombination and found that RAG2, PRKDC, LIG4, and NHEJ1 genes were highly associated with it, suggesting that these genes may be suggestive for future studies on the immunological aspects of OSA pathogenesis.

As for the pathway analysis, the pathways in cancer, the focal adhesion, and the proteoglycans in cancer might play important roles in the development of heart injury caused by OSA. Recent studies suggest that cardiac disease development may involve dysregulated endocardial cell migration [35]. Paluch et al. showed the focal adhesion pathway is thought to be associated with cell migration [36]. Focal adhesions serve as critical anchoring points between cells and the extracellular matrix, enabling the transmission of mechanical forces that drive cell migration in two-dimensional (2D) environments. The AMPK pathway plays a pivotal role in mitigating cardiac microvascular ischemia/reperfusion (I/R) injury by activating LKB1/AMPK/ULK1-mediated autophagy, which promotes STING degradation and suppresses apoptosis [37]. Our data suggest that this pathway may be involved in OSA-induced cardiac injury. The results of these enrichment analyses give us a basis for our future exploration between OSA and the pathogenesis of cardiovascular system lesions.

In the past few years, ceRNAs have emerged as an important class of transcriptional regulators involved in the development of many diseases [38–40]. As a subclass of ceRNA, circRNAs have been reported to function primarily as miRNA sponges in many biological processes [41]. There have been some studies reporting regulatory relationships between circRNAs, miRNAs, and target genes. For instance, Zhang N et al. reported that the overexpression of circ-ITCH protected cardiomyocytes by inhibiting apoptosis, whereas miR-17-5p increased apoptosis and inhibited cell viability via the Wnt/-catenin signaling pathway [42].Shan B et al. discovered that miR-93-5p protects myocardial cells by being regulated by H19, which sponges miR-93-5p to promote SORBS2 expression. This interaction helps reverse LPS-induced cell growth inhibition, mitochondrial damage, and inflammatory responses, thereby attenuating sepsis-induced myocardial injury [43]. Notably, the relationship between circRNAs with m6A peaks and the pathogenesis of cardiovascular disease has not been elucidated.

Therefore, we predicted a ceRNA network in our study. We found that mmu_circRNA_22543 was further predicted to have pathway linkage with miRNA such as mmu-miR-5134-5p, mmu-miR-1896, and mmu-miR-7242-3p and their corresponding targeted genes. Of interest to us, Hu et al. reported that high expression of Clip2 allows oxidatively modified LDL to stimulate lipid accumulation in THP-1 macrophages and promote foam cell formation, implying that high expression of this gene may have an important role in heart damage [44]. The correlation between mmu_circRNA_22543 and the Clip2 gene is suggested by our network, which means that the pathogenic bridge between m6A-modified circRNAs and cardiac injury may be the excessive accumulation of lipids and the massive formation of foam cells. Our ceRNA network analysis revealed a potential link between mmu_circRNA_22543 and lipid metabolism via the Clip2 gene, suggesting a previously unrecognized mechanism in OSA-induced cardiac damage. The construction of CNC networks and the analysis of relevant targeted genes may be vital steps for us to study the pathogenesis of cardiovascular disease caused by OSA.

However, some limitations should be recognized in the study. Firstly, due to the limited number of circRNAs with m6A peaks identified in this study, the comprehensiveness of the results may be difficult to ascertain. In the meantime, to ascertain the appropriate sample size for the experiment, power analysis should be conducted. And the sample size should be expanded as much as possible to improve the reliability of the experiment. Secondly, our study explores the pathways and targets that these candidate circRNAs may be involved in the

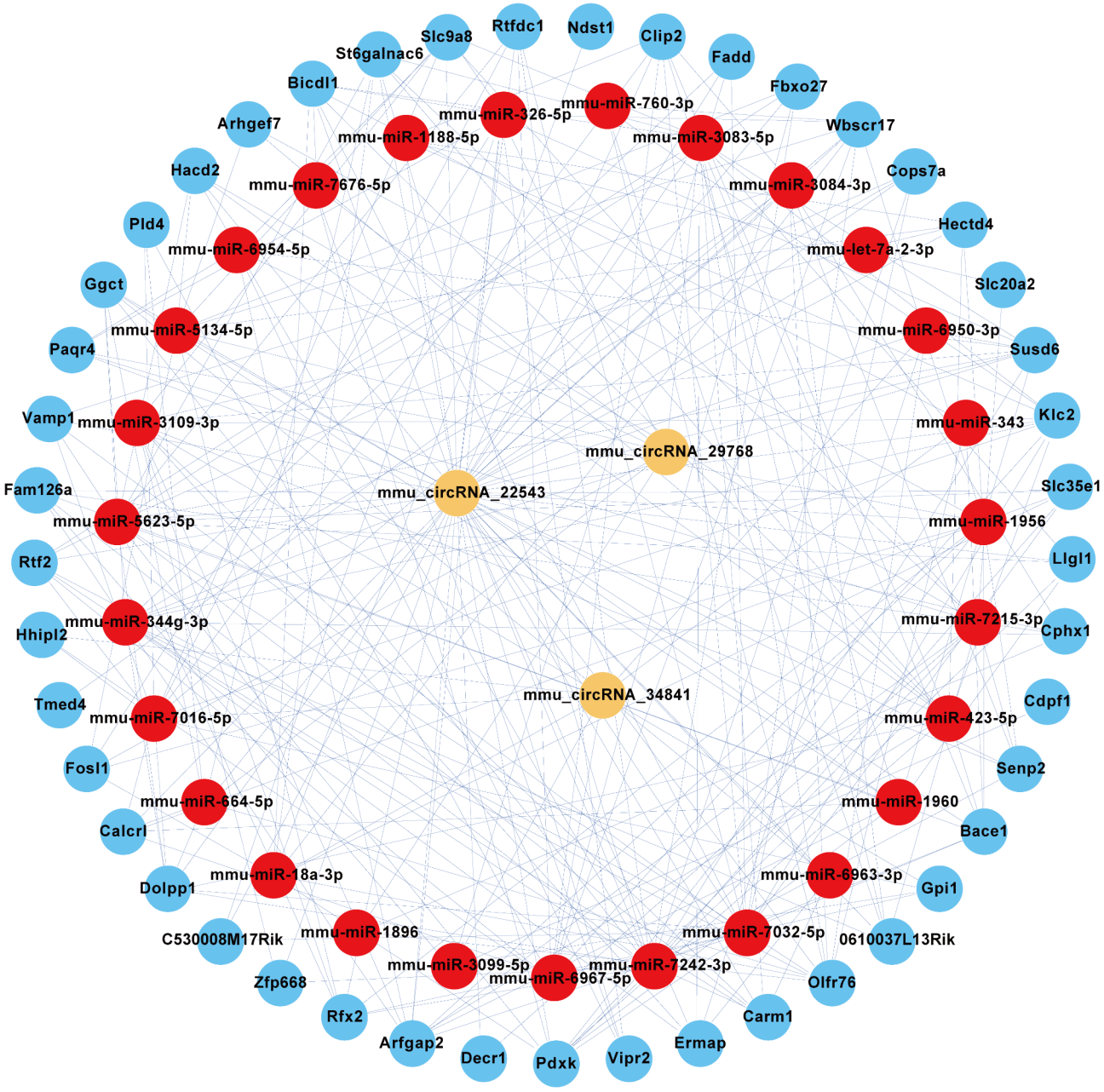

Fig. 6 ceRNA Network of m6A-modified circRNAs in OSA-induced Cardiac Injury. The ceRNA network demonstrates the interactions between m6A-modified circRNAs, miRNAs, and their target mRNAs in the context of OSA-induced myocardial injury. Key circRNAs identified, including mmu_circRNA_22543, mmu_circRNA_29768, and mmu_circRNA_34841, are shown in the network, interacting with miR-5134-5p, miR-1896, and other miRNAs. These miRNAs regulate downstream target genes such as Clip2, Fadd, and Hacd2, which are involved in myocardial injury and heart disease pathways. The figure highlights the potential regulatory role of these circRNAs in modulating gene expression through miRNA sponging, impacting key cellular processes like inflammation and fibrosis in OSA-induced cardiac injury. The arrows represent direct interactions, with color coding indicating the strength of correlation, and the size of nodes indicating the importance of each gene in the network

pathogenesis of heart injury caused by OSA, rather than investigating the exact mechanism. Therefore, more epigenetic research is needed to determine the precise regulatory mechanisms of m6A-modified circRNAs in OSA-induced myocardial injury. Thirdly, despite mice and human genomes being highly homologous, further research and confirmation are needed to see if the results we have obtained in mice can be applied to humans.

Our future work is structured into three integrated layers to elucidate the functional roles and therapeutic potential of m6A-modified circRNAs in OSA-induced cardiac injury. First, in cell models, we will investigate key m6A-modified circRNAs in human cardiomyocyte

cell lines under IH conditions mimicking OSA. Using RNAi, we will knockdown selected circRNAs and assess their effects on proliferation, apoptosis, and inflammation, while luciferase reporter assays will validate circRNA-miRNA-mRNA interactions to uncover regulatory mechanisms. Second, in animal models, we will expand OSA-induced cardiac injury studies in mice, employing gain- and loss-of-function strategies, such as circRNA overexpression or knockdown via AAV or RNAi, to evaluate their impact on cardiac function and injury, determining their protective or detrimental roles. We will also explore the therapeutic potential of circRNAs by assessing their ability to mitigate cardiac damage and improve heart function. Third, bioinformatics and pathway validation will utilize pathway inhibitors and gene silencing to validate key pathways identified through GO and KEGG analyses, clarifying how m6A-modified circRNAs regulate signaling pathways in cardiac injury progression. Together, these multi-layered studies aim to bridge preclinical findings with clinical applications, uncovering circRNA-based therapeutic strategies for OSA-related cardiovascular diseases.

Conclusion

In summary, our study provides the first proof that m6A-modified circRNAs have different expression levels in the onset and progression of cardiac injury caused by OSA. Then we predict their biological significance as well as potential targets and pathways. These findings could provide new insights into the possible pathologic and physiological mechanisms of cardiac injury caused by OSA and assist in seeking novel therapeutic approaches.

Abbreviations

OSA	Obstructive sleep apnea
CircRNAs	Circular RNAs
m6A	N6-methyladenosine
CIH	Chronic intermittent hypoxia
GO	Gene Ontology
KEGG	Kyoto Encyclopedia of Genes and Genomes

Acknowledgements

The authors thanked KangChen Bio-tech (Shanghai, China) for the microarray work.

Author contributions

QC designed the study, JL, CL, and HC established the mouse models and conducted the statistical analysis. JL and YW wrote the manuscript. QC revised the manuscript. All authors read and approved the final manuscript.

Funding

This project was supported by the Joint Funds for the innovation of science and Technology, Fujian province (Grant number: 2021Y9027), Science and Technology Bureau of Quanzhou (Grant number: 2022C038R), Young and middle-aged backbone talents training project of Fujian Provincial Health Commission (Grant number: 2021GGA040), Doctoral Miaopu project of the Second Affiliated Hospital of Fujian Medical University (Grant number: BS202115), Fujian Provincial Natural Science Foundation of China (Grant number: 2024J01662), and the National Natural Science Foundation of China (Grant number: 82000094).

Data availability

The datasets generated and analysed during the current study are available in the GEO repository, https://www.ncbi.nlm.nih.gov/geo/query/acc.cgi?acc=GSE224632, enter token into the box is cnebegmifxibtaz.

Declarations

Ethics approval and consent to participate

All methods were performed in accordance with relevant guidelines and regulations. The animal protocol for this work was approved by the Second Affiliated Hospital of Fujian Medical University's Experimental Animal Ethics Committee (Number: 2022FYFELL15). Animal procedures were complied with the ARRIVE 2.0 guidelines.

Consent for publication

Not applicable.

Competing interests

The authors declare no competing interests.

Received: 26 December 2023 / Accepted: 19 March 2025
Published online: 05 April 2025

References

1. Yeghiazarians Y, Jneid H, Tietjens JR, Redline S, Brown DL, El-Sherif N, Mehra R, Bozkurt B, Ndumele CE, Somers VK. Obstructive sleep apnea and cardiovascular disease: A scientific statement from the American heart association. Circulation. 2021;144(3):e56–67.
2. Arnaud C, Bochaton T, Pépin J-L, Belaidi E. Obstructive sleep Apnoea and cardiovascular consequences: pathophysiological mechanisms. Arch Cardiovasc Dis. 2020;113(5):350–8.
3. Ismail K, Roberts K, Manning P, Manley C, Hill NS. OSA and pulmonary hypertension: time for a new look. Chest. 2015;147(3):847–61.
4. Gottlieb DJ. Sleep apnea and cardiovascular disease. Curr Diab Rep. 2021;21(12):64.
5. May AM, Van Wagoner DR, Mehra R. OSA and cardiac arrhythmogenesis: mechanistic insights. Chest. 2017;151(1):225–41.
6. Qu S, Yang X, Li X, Wang J, Gao Y, Shang R, Sun W, Dou K, Li H. Circular RNA: A new star of noncoding RNAs. Cancer Lett. 2015;365(2):141–8.
7. Meng X, Li X, Zhang P, Wang J, Zhou Y, Chen M. Circular RNA: an emerging key player in RNA world. Brief Bioinform. 2017;18(4):547–57.
8. Rong D, Sun H, Li Z, Liu S, Dong C, Fu K, Tang W, Cao H. An emerging function of circRNA-miRNAs-mRNA axis in human diseases. Oncotarget. 2017;8(42):73271–81.
9. Xin Z, Ma Q, Ren S, Wang G, Li F. The Understanding of circular RNAs as special triggers in carcinogenesis. Brief Funct Genomics. 2017;16(2):80–6.
10. Sygitowicz G, Sitkiewicz D. Involvement of circrnas in the development of heart failure. Int J Mol Sci. 2022, 23(22).
11. Hu L, Wu W, Zou J. Circular RNAs: typical biomarkers for bone-related diseases. J Zhejiang Univ Sci B. 2022;23(12):975–88.
12. Kumari R, Ranjan P, Suleiman ZG, Goswami SK, Li J, Prasad R, Verma SK. mRNA modifications in cardiovascular biology and disease: with a focus on m6A modification. Cardiovasc Res. 2022;118(7):1680–92.
13. Zhao BS, Roundtree IA, He C. Post-transcriptional gene regulation by mRNA modifications. Nat Rev Mol Cell Biol. 2017;18(1):31–42.
14. Wang T, Kong S, Tao M, Ju S. The potential role of RNA N6-methyladenosine in cancer progression. Mol Cancer. 2020;19(1):88.
15. Zhang Z, Park E, Lin L, Xing Y. A panoramic view of RNA modifications: exploring new frontiers. Genome Biol. 2018;19(1):11.
16. Jia G, Fu Y, He C. Reversible RNA adenosine methylation in biological regulation. Trends Genet. 2013;29(2):108–15.
17. Liao S, Sun H, Xu C. YTH domain: A family of N-methyladenosine (mA) readers. Genomics Proteom Bioinf. 2018, 16(2).
18. Ianniello Z, Fatica A. N6-Methyladenosine role in acute myeloid leukaemia. Int J Mol Sci. 2018, 19(8).
19. Hunyor I, Cook KM. Models of intermittent hypoxia and obstructive sleep apnea: molecular pathways and their contribution to cancer. Am J Physiol Regul Integr Comp Physiol. 2018;315(4):R669–87.

20. Javaheri S, Barbe F, Campos-Rodriguez F, Dempsey JA, Khayat R, Javaheri S, Malhotra A, Martinez-Garcia MA, Mehra R, Pack AI, et al. Sleep apnea: types, mechanisms, and clinical cardiovascular consequences. J Am Coll Cardiol. 2017;69(7):841–58.
21. Whelton PK, Carey RM, Aronow WS, Casey DE, Collins KJ, Dennison Himmelfarb C, DePalma SM, Gidding S, Jamerson KA, Jones DW et al. 2017 ACC/AHA/AAPA/ABC/ACPM/AGS/APhA/ASH/ASPC/NMA/PCNA Guideline for the prevention, detection, evaluation, and management of high blood pressure in adults: A report of the American college of Cardiology/American heart association task force on clinical practice guidelines. J Am Coll Cardiol. 2018;71(19):e127-e248.
22. Vanek J, Prasko J, Genzor S, Ociskova M, Kantor K, Holubova M, Slepecky M, Nesnidal V, Kolek A, Sova M. Obstructive sleep apnea, depression and cognitive impairment. Sleep Med. 2020;72:50–8.
23. Schütz SG, Dunn A, Braley TJ, Pitt B, Shelgikar AV. New frontiers in Pharmacologic obstructive sleep apnea treatment: A narrative review. Sleep Med Rev. 2021;57:101473.
24. Zhong Y, Du Y, Yang X, Mo Y, Fan C, Xiong F, Ren D, Ye X, Li C, Wang Y, et al. Circular RNAs function as CeRNAs to regulate and control human cancer progression. Mol Cancer. 2018;17(1):79.
25. Garikipati VNS, Verma SK, Cheng Z, Liang D, Truongcao MM, Cimini M, Yue Y, Huang G, Wang C, Benedict C, et al. Circular RNA CircFndc3b modulates cardiac repair after myocardial infarction via FUS/VEGF-A axis. Nat Commun. 2019;10(1):4317.
26. Ge X, Meng Q, Zhuang R, Yuan D, Liu J, Lin F, Fan H, Zhou X. Circular RNA expression alterations in extracellular vesicles isolated from murine heart post ischemia/reperfusion injury. Int J Cardiol. 2019;296:136–40.
27. Zhou C, Molinie B, Daneshvar K, Pondick JV, Wang J, Van Wittenberghe N, Xing Y, Giallourakis CC, Mullen AC. Genome-Wide maps of m6A circrnas identify widespread and Cell-Type-Specific methylation patterns that are distinct from mRNAs. Cell Rep. 2017;20(9):2262–76.
28. Chen R-X, Chen X, Xia L-P, Zhang J-X, Pan Z-Z, Ma X-D, Han K, Chen J-W, Judde J-G, Deas O, et al. N6-methyladenosine modification of circNSUN2 facilitates cytoplasmic export and stabilizes HMGA2 to promote colorectal liver metastasis. Nat Commun. 2019;10(1):4695.
29. Di Timoteo G, Dattilo D, Centrón-Broco A, Colantoni A, Guarnacci M, Rossi F, Incarnato D, Oliviero S, Fatica A, Morlando M, et al. Modulation of circrna metabolism by m6A modification. Cell Rep. 2020;31(6):107641.
30. Yang Y, Fan X, Mao M, Song X, Wu P, Zhang Y, Jin Y, Yang Y, Chen L-L, Wang Y, et al. Extensive translation of circular RNAs driven by N6-methyladenosine. Cell Res. 2017;27(5):626–41.
31. Park OH, Ha H, Lee Y, Boo SH, Kwon DH, Song HK, Kim YK. Endoribonucleolytic cleavage of m6A-Containing RNAs by RNase P/MRP complex. Mol Cell. 2019, 74(3).
32. Chen YG, Chen R, Ahmad S, Verma R, Kasturi SP, Amaya L, Broughton JP, Kim J, Cadena C, Pulendran B et al. N6-Methyladenosine modification controls circular RNA immunity. Mol Cell 2019, 76(1).
33. Tang C, Xie Y, Yu T, Liu N, Wang Z, Woolsey RJ, Tang Y, Zhang X, Qin W, Zhang Y, et al. m6A-dependent biogenesis of circular RNAs in male germ cells. Cell Res. 2020;30(3):211–28.
34. Berulava T, Buchholz E, Elerdashvili V, Pena T, Islam MR, Lbik D, Mohamed BA, Renner A, von Lewinski D, Sacherer M, et al. Changes in m6A RNA methylation contribute to heart failure progression by modulating translation. Eur J Heart Fail. 2020;22(1):54–66.
35. Gunawan F, Priya R, Stainier DYR. Sculpting the heart: cellular mechanisms shaping valves and trabeculae. Curr Opin Cell Biol. 2021;73:26–34.
36. Paluch EK, Aspalter IM, Sixt M. Focal Adhesion-Independent cell migration. Annu Rev Cell Dev Biol. 2016;32:469–90.
37. Liu W, Hu J, Wang Y, Gan T, Ding Y, Wang X, Xu Q, Xiong J, Xiong N, Lu S, et al. 9-PAHSA ameliorates microvascular damage during cardiac ischaemia/reperfusion injury by promoting LKB1/AMPK/ULK1-mediated autophagy-dependent STING degradation. Phytomedicine. 2025;136:156241.
38. Ma N, Tie C, Yu B, Zhang W, Wan J. Identifying lncRNA-miRNA-mRNA networks to investigate Alzheimer's disease pathogenesis and therapy strategy. Aging. 2020;12(3):2897–920.
39. Long J, Bai Y, Yang X, Lin J, Yang X, Wang D, He L, Zheng Y, Zhao H. Construction and comprehensive analysis of a CeRNA network to reveal potential prognostic biomarkers for hepatocellular carcinoma. Cancer Cell Int. 2019;19:90.
40. Li B, Li Y, Hu L, Liu Y, Zhou Q, Wang M, An Y, Li P. Role of circular RNAs in the pathogenesis of cardiovascular disease. J Cardiovasc Transl Res. 2020;13(4):572–83.
41. Misir S, Hepokur C, Aliyazicioglu Y, Enguita FJ. Circular RNAs serve as MiRNA sponges in breast cancer. Breast Cancer. 2020;27(6):1048–57.
42. Zhang N, Wang X. Circular RNA ITCH mediates H2O2-induced myocardial cell apoptosis by targeting miR-17-5p via wnt/β-catenin signalling pathway. Int J Exp Pathol. 2020;102(1):22–31.
43. Shan B, Li JY, Liu YJ, Tang XB, Zhou Z, Luo LX. LncRNA H19 inhibits the progression of Sepsis-Induced myocardial injury via regulation of the miR-93-5p/SORBS2 axis. Inflammation. 2021;44(1):344–57.
44. Hu W, Li K, Han H, Geng S, Zhou B, Fan X, Xu S, Yang M, Liu H, Yang G et al. Circulating Levels of CILP2 Are Elevated in Coronary Heart Disease and Associated with Atherosclerosis. Oxid Med Cell Longev. 2020;2020:1871984.

Publisher's note